Synthesis of Au-130(SR)(50) and Au130-xAgx(SR)(50) nanomolecules through core size conversion of larger metal clusters

ARTICLE *in* PHYSICAL CHEMISTRY CHEMICAL PHYSICS · APRIL 2014

Impact Factor: 4.49 · DOI: 10.1039/c3cp54343a · Source: PubMed

2 AUTHORS, INCLUDING:

Amala Dass
University of Mississippi
108 PUBLICATIONS **3,285** CITATIONS

SEE PROFILE

PCCP

PAPER

Synthesis of $Au_{130}(SR)_{50}$ and $Au_{130-x}Ag_x(SR)_{50}$ nanomolecules through core size conversion of larger metal clusters†

Cite this: *Phys. Chem. Chem. Phys.*, 2014, **16**, 10473

Vijay Reddy Jupally and Amala Dass*

Received 14th October 2013,
Accepted 31st March 2014

DOI: 10.1039/c3cp54343a

www.rsc.org/pccp

Gold nanomolecules with a precise number of metal atoms and thiolate ligands are being used for catalysis, biosensing, drug delivery and as alternative energy sources. Highly monodisperse products, with reproducible synthesis and complete characterization, are essential for these purposes. Post synthetic etching is used to synthesize highly stable gold nanomolecules. We report a synthetic protocol for the scalable synthesis of $Au_{130}(SR)_{50}$ for the first time, by etching of larger clusters *via* a core conversion process. $Au_{130}(SR)_{50}$ is not present in the crude product, but, is exclusively formed by etching larger clusters (>40 kDa). This is the first evidence that larger nanocluster cores convert to $Au_{130}(SR)_{50}$. The special stability of $Au_{130}(SR)_{50}$ is confirmed by the formation of $Au_{130-x}(metal)_x(SR)_{50}$, where R = CH_2CH_2Ph, C_6H_{13}, $C_{12}H_{25}$ and metal = Ag, Pd. $Au_xAg_{130-x}(SR)_{50}$ is isolated and characterized with two different Au : Ag precursor ratios. Upon alloying there is a change in the optical features of this 130-metal atom nanomolecule. To understand the process of etching and core conversion, a possible mechanism is being proposed. Highly stable nanomolecules like this can find potential applications in high temperature catalysis and sensing.

Introduction

Novel nanomaterials with tunable physical and chemical properties are finding increasing applications in drug delivery,[1] biosensors,[2] catalysis[3] and other applications.[4,5] Gold nanomolecules contain a precise number of gold atoms and ligands, can be isolated in a dried form and redispersed in solvents.[6] The properties of gold nanomolecules can be tuned due to their size, shape and composition dependence.[6] Put together with reproducible synthesis and characterization, these materials find several applications as mentioned above. Pure nanomolecules, with high yield synthetic routes, are essential for this purpose.

Organothiolate gold nanomolecules are typically synthesized using the two-phase Brust–Schiffrin[7] method resulting in polydisperse products. *Etching* narrows down the size distribution of these polydisperse samples by eliminating the metastable species. Such a concept originated from Self Assembled Monolayers (SAMs),[8] where the surface gold atoms are lost when the thiols are absorbed onto the SAM surface. Whetten extended this concept of etching[9] to gold nanomolecules, which are 3D analogues of SAMs.[10] Recently, Murray's and Tsukuda's groups used etching to synthesize $Au_{144}(SR)_{60}$ and $Au_{38}(SR)_{24}$.[11,12] This well established method with a long history was described recently as 'size focusing'.[13,14]

Nanomolecules with size less than 100 atoms were the main focus of etching until recently. We recently reported several sizes larger than $Au_{144}(SR)_{60}$ prepared by etching larger sized polydisperse samples.[15] Negishi reported $Au_{130}(SR)_{50}$ and $Au_{187}(SR)_{68}$ nanomolecules, prepared by etching and analytical SEC separation of millimolar concentrations of nanoclusters.[16] We have observed $Au_{130}(SR)_{50}$ always accompanied by $Au_{144}(SR)_{60}$, in the ESI mass spectrum of phenylethanethiol based synthesis in the past five years over 100 times indicating the reproducible formation of $Au_{130}(SR)_{50}$ in a wide variety of synthetic conditions. The separation of $Au_{130}(SR)_{50}$ from $Au_{144}(SR)_{60}$ was not feasible until now. In this report, we have etched clusters larger than 40 kDa (no Au_{144} present) with excess thiol at 80 °C. The $Au_{130}(SR)_{50}$ nanomolecule is formed in such reactions in large quantities. This is a clear result of *core conversion* of larger nanomolecules, that is, $Au_{130}(SR)_{50}$ is not present in the initial crude mixture, but is exclusively formed *via* core size conversion of clusters larger than ~150 gold atoms. Here, we isolated pure $Au_{130}(SR)_{50}$ in a preparative scale using a SEC column chromatography method, by eliminating $Au_{144}(SR)_{60}$ from the starting crude mixture. Gangli Wang and coworkers have also reported a compound in the 130 metal atom range comprising both mono- and di-thiols.[17]

Department of Chemistry and Biochemistry, University of Mississippi, MS 38677, USA. E-mail: amal@olemiss.edu

† Electronic supplementary information (ESI) available: Additional mass spectrometry and UV-vis spectroscopy data. See DOI: 10.1039/c3cp54343a

Formed by the core size conversion of larger nanoclusters, the $Au_{130}(SR)_{50}$ nanomolecule is very stable at temperatures as high as 85 °C. The *special stability* of the nanomolecule is indicated by the formation of $Au_{130-x}(metal)_x(SR)_{50}$, where R = CH_2CH_2Ph, C_6H_{13}, $C_{12}H_{25}$ and metal = Ag, Pd. Though $Au_{130}(SR)_{50}$ has been reported before using a small scale analytical HPLC column separation, no clear synthetic route is available so far to synthesize the nanomolecule in large quantities. Here we report a synthetic route, *via* a core conversion process, (a) to make $Au_{130}(SR)_{50}$ in scalable quantities, (b) to eliminate the interference of $Au_{144}(SR)_{60}$ during SEC separation, (c) to synthesize Au–Ag alloy systems and Au–Pd alloy systems of this 130 metal atom species. Also, $Au_xAg_{130-x}(SR)_{50}$ with two different Au : Ag precursor ratios was isolated and characterized in this work. Further insights into the mechanism of core size conversion are also presented here.

Experimental methods

Chemicals

Phenylethanemercaptan (SAFC, ≥99%), hexanethiol (Fluka), *n*-butanethiol (Acros), sodium borohydride (Acros, 99%), and *trans*-2-[3(4-tertbutylphenyl)-2-methyl-2-propenylidene]malononitrile (DCTB matrix) (Fluka ≥99%) were used as received. Tetrahydrofuran (stabilized) and other solvents like toluene, methanol, acetonitrile and acetone were used from Fisher as received. Biorad-SX1 beads from Biorad were used for the SEC.

Equipment

UV-visible absorption spectra were recorded in toluene on a Shimadzu UV-1601 spectrophotometer. Matrix assisted laser desorption ionization (MALDI) time-of-flight mass spectra were collected on a Bruker Autoflex mass spectrometer in linear positive mode using a nitrogen laser (337 nm) with DCTB as a matrix. ESI-MS spectra were acquired using a Waters SYNAPT HDMS instrument. Powder XRD measurements were performed on a Bruker D8-Focus XRD instrument on a quartz substrate. 8 mg of sample was dissolved in a minimal amount of toluene and deposited on the substrate and air-dried prior to the measurements.

Synthesis of the crude material

0.35 g (0.88 mmol) of $HAuCl_4$ dissolved in 20 mL of distilled water was added to 0.6 g (1.1 mmol) TOABr in 30 mL toluene in a round bottom flask. The contents were mixed for 30 min at 500 rpm until all the gold salt transferred to the organic layer. Then, stirring was ceased and the contents were transferred into a beaker. The reaction flask was cleaned with acetone and air-dried. The organic layer was then transferred into the reaction flask and 0.112 mL (0.88 mmol) of phenylethanethiol was added and stirred for 30 min at 500 rpm. For the next 30 min, the reaction flask was transferred into an ice bath while the stirring was continued. 0.75 (19.8 mmol) g of $NaBH_4$ in 20 mL ice-cold distilled water was added to the reaction mixture instantaneously. Upon addition of $NaBH_4$, the reaction mixture turned dark, indicating the formation of nanoparticles. The reaction was stopped after 3 h of sodium borohydride addition. The aqueous layer was pipetted out and the contents were dried by rotary evaporation. The resulting product was washed with methanol three times by centrifugal precipitation and dried by rotary evaporation. The resulting products were analyzed by MALDI-TOF MS. For synthesizing a crude product with Au–Ag, the same procedure was followed except that different ratios of Au : Ag were used instead of $HAuCl_4$ alone.

Solvent fractionation

Toluene–THF and methanol were used for all the solvent fractionation steps. In the solvent fractionation step, the contents were first dissolved in about 1 to 1.5 mL of toluene or THF and methanol was added slowly using a pipette. Once the precipitate was observed in the vial, the contents were centrifuged and the supernatant was separated from the precipitate. This step should be done carefully to avoid cross contamination between the supernatant and the precipitate. The separated fractions were then analyzed by MALDI-MS for the first estimate of the separation. The purpose of solvent fractionation is to isolate clusters larger than 40 kDa (>40 kDa sample) and etch it. This will ensure the absence of 144-atom clusters, eliminating the need for the difficult separation of 130-atom species from 144-atom species. The same procedure was used for isolation of the >40 kDa sample from the Au–Ag crude product.

Thermochemical treatment of the clusters >40 kDa

To the >40 kDa sample obtained after solvent fractionation (200 mg), 0.800 mL of phenylethanethiol was added and heated at 85 °C and 300 rpm. To monitor the progress of the reaction, aliquots from the reaction were collected with time, washed with methanol by centrifugal precipitation, and analyzed by MALDI-TOF MS. The etching was stopped when the 32 kDa cluster (130-atom species) was the most dominant species in the MALDI spectra. Scheme 1 shows the several steps involved in the synthesis of $Au_{130}(SR)_{50}$.

Size exclusion chromatography

SX1 beads from Biorad were soaked in stabilized THF overnight. Stabilized THF was used as an eluent and various fractions were collected.[18] The fractions were analyzed by MALDI-TOF to determine the composition. 20 mg of $Au_{130}(SR)_{50}$ and 12 mg of $Au_{130-x}Ag_x(SR)_{50}$ was obtained per 300 mg batch of $HAuCl_4$ starting material. The yield of a typical core size conversion reaction is 8.5% to 10.5% on Au atom basis. The yield for Au–Ag

Scheme 1 The various steps involved in the synthesis of $Au_{130}(SR)_{50}$.

reactions was not calculated as the total amount of Ag present in the alloy samples cannot be determined quantitatively.

Results and discussion

I. Core size conversion of larger (>40 kDa) clusters

Polydisperse samples are reacted with excess thiol at elevated temperatures during etching.[9] Stable core sizes survive the process while the metastable ones perish. Similar results were reported for gold clusters with phosphine ligands.[19] Also, clusters of several other metals were synthesized using this method. To obtain pure $Au_{130}(SR)_{50}$, clusters >40 kDa were etched in excess thiol at 85 °C. Typically 100 mg of sample was etched with 0.4 mL of thiol. Fig. 1 shows the progress of the etching reaction with time monitored by MALDI-TOF mass spectrometry. The crude mixture at 0 h contains clusters larger than 40 kDa with no $Au_{130}(SCH_2CH_2Ph)_{50}$ or $Au_{144}(SCH_2CH_2Ph)_{60}$. To show this, an expanded spectrum of the crude product in the $Au_{130}(SCH_2CH_2Ph)_{50}$ mass region is presented in Fig. S1 in the ESI.† With time, a new core sized nanomolecule, $Au_{130}(SCH_2CH_2Ph)_{50}$, is formed which was not present in the initial product. Mass spectrometry data show the accumulation of $Au_{130}(SCH_2CH_2Ph)_{50}$ with time in the reaction mixture. This clearly shows that larger clusters (>40 kDa) are core converted to form $Au_{130}(SCH_2CH_2Ph)_{50}$. The stability of Au_{144} and Au_{137} should be mentioned at this point. When the crude products from the synthesis are etched prior to the isolation of clusters larger than 40 kDa, a mixture of Au_{130}, Au_{137} and Au_{144} is obtained. This suggests the stability of Au_{144} and Au_{137} nanomolecules during etching. It should be noted that the etching of clusters smaller than Au_{144} give Au_{38}, Au_{137} and Au_{144} as the final products, reinforcing the same point that Au_{137} and Au_{144} are stable during the etching process.

At 12 h, some meta-stable clusters still exist in the reaction mixture so the etching is continued. The meta-stable clusters were found at 43.6, 89.2, 113.3 and 140.7 kDa corresponding to ~220, 450, 570, and 710-atom species. After about 36 h, the MALDI spectrum is dominated by a peak at ~32 kDa (130-atom nanomolecules). The reaction is stopped after 48 h and processed. The time frame of the reaction is dependent on the initial product and varies for different reactions. A previously reported 76.3 kDa nanomolecule (~320-atoms) is also observed in these reactions.[15,20] A 32 kDa species was isolated using size exclusion chromatography (SEC) and analyzed by ESI-MS. From the ESI-MS data, the nanomolecule was confirmed to be $Au_{130}(SR)_{50}$. The core size conversion from >40 kDa clusters to $Au_{130}(SR)_{50}$ was confirmed in various reactions where different ligands were employed. These results are presented in Fig. S2–S4 in ESI.† The etching of larger clusters with either phenylethanethiol, hexanethiol or dodecanethiol resulted in the formation of $Au_{130}(SR)_{50}$ by core size conversion as shown in Fig. 2. Note that the synthesis and etching was carried out using the same ligand.

The molecular weight of $Au_{130}(SCH_2CH_2Ph)_{50}$ is 32 467 Da. MALDI-TOF MS generally produces 1+ ions and therefore shows peaks in the 32 kDa region. However the peaks at this high mass region are generally broad, with a fwhm of 1000 m/z as shown in Fig. 1. This makes the MALDI spectrum unsuitable for determination of composition, in terms of the number of Au atoms and ligands. Electrospray ionization mass spectrometry (ESI-MS) generally yields multiply charged peaks. As these multiply charged peaks appear at a lower mass range, they are better resolved than the molecular ions, thereby allowing the assignment of composition of nanomolecules. Fig. 2 shows the 3+ region of the $Au_{130}(SCH_2CH_2Ph)_{50}$ nanomolecules,

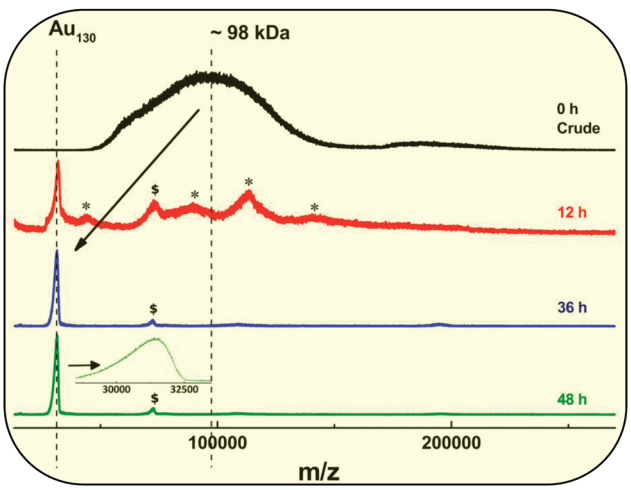

Fig. 1 MALDI mass spectra of the samples collected at several time intervals from etching of larger (>40 kDa) clusters. Note that (1) $Au_{130}(SR)_{50}$ is absent initially. $Au_{130}(SR)_{50}$ is formed by the core size conversion of larger (>~200 atom) nanoclusters, (2) $Au_{144}(SR)_{60}$ is not present in the starting material or in the final product. So $Au_{144}(SR)_{60}$ is not a product of core size conversion in this study. The absence of $Au_{144}(SR)_{60}$ in the final product enables the preparative scale SEC separation and isolation of pure $Au_{130}(SR)_{50}$. Asterisks indicate metastable clusters. The peak labeled $ in 12 h, 36 h and 48 h samples corresponds to the 76.3 kDa nanomolecule,[15] which is stable throughout the etching process.

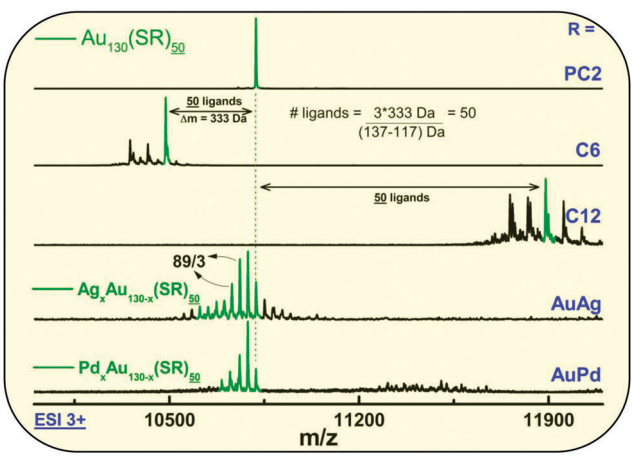

Fig. 2 Positive mode ESI-MS mass spectra showing the 3+ region of $Au_{130}(SR)_{50}$ with several ligands phenylethanethiol (PC2), hexanethiol (C6), dodecanethiol (C12), $Au_{130-x}Ag_x(SR)_{50}$ and $Au_{130-x}Pd_x(SR)_{50}$. The purpose of this figure is to show that (a) the core size conversion works with various ligands and alloy systems, (b) the 130-atom core has special stability associated with its structure.

at 10 822 m/z (32 467/3). Fig. 2 shows all the different $Au_{130-x}(metal)_x(SR)_{50}$ nanomolecules prepared, where R = $-CH_2CH_2Ph$, $-C_6H_{13}$, $-C_{12}H_{25}$ and metal = Pd and Au. Using the mass difference between the peaks corresponding to $Au_{130}(SR)_{50}$ with phenylethanethiol, hexanethiol and dodecanethiol, the number of ligands was calculated. In both hexanethiol and dodecanethiol ligands, the number of ligands was confirmed to be 50, which adds confidence to the assignment. This also confirms that $Au_{130}(SR)_{50}$ is the product of core conversion in all three ligand systems. Compositional isomers, in short "*Composomers*", of this 130-metal atom nanomolecule were prepared by the same core size conversion method. Composomers have the same number of total metal atoms and ligands, while the numbers of individual type of metal atoms vary.[21] $Au_{116}Ag_{14}(SR)_{50}$ and $Au_{118}Ag_{12}(SR)_{50}$ are examples for 130-metal atom composomers. Here, the total number of metal atoms is 130. But the numbers of gold and silver atoms vary. Several alloy nanomolecules are evident in the literature.[22–27]

II. Core size conversion in AuAg alloy nanoclusters

The core size conversion process is also tested in the alloy systems as mentioned before. In the past, our group reported the synthesis of $Au_{144-x}Ag_x(SR)_{60}$ and $Au_{38-x}Ag_x(SR)_{24}$.[23,24] Using the same synthetic protocol, a crude product was synthesized. Then, clusters larger than 40 kDa were isolated and etched. Upon etching, $Au_{130-x}Ag_x(SR)_{50}$ was formed in the reactions. This indicates the validity of the core size conversion phenomenon in alloy systems. Fig. 3 shows the positive mode ESI MS of $Au_{130-x}Ag_x(SR)_{50}$ formed at two different Au : Ag precursor ratios. At 1 : 0.1 Au : Ag ratio, $Au_{130}(SCH_2CH_2Ph)_{50}$ is the major peak in ESI MS with about a maximum of 3 silver atom incorporations. When the Au : Ag ratio was increased to 1 : 0.15, the number of silver atoms incorporated increased with $Au_{125}Ag_5(SCH_2CH_2Ph)_{50}$ being the most intense peak. But the maximum number of silver atom incorporations was 20. With a Au : Ag ratio of 1 : 0.1, some peaks to the left of $Au_{130}(SR)_{50}$ were observed. These are assigned to metal cores comprising of 131 atoms, as shown in Fig. S10 in the ESI.† Upon further increase in the Au : Ag precursor ratios, there was no $Au_{130-x}Ag_x(SR)_{50}$ observed in the reaction mixtures. This could be because of the instability of the 130 atom clusters upon increased silver incorporation. Similar stability issues with higher silver incorporations were also observed for $Au_{144-x}Ag_x(SR)_{60}$ and $Au_{38-x}Ag_x(SR)_{24}$. However, the fact that the 130 metal atom composition allows alloying with silver atoms to an extent indicates the high stability, which in turn is a result of the geometry and structure. The doping of gold nanomolecules with palladium, platinum and silver has been reported to increase the stability and catalytic activity. Here we note that the composition of $Au_{130}(SR)_{50}$ has been reported recently by the Negishi group.[16] The purpose of this work and the preparation of 130-atom nanomolecule composomers is to (a) establish a synthetic protocol for scalable synthesis, (b) demonstrate the reproducibility of the core-size conversion process, (c) show the special stability of 130-atom core under various conditions like high temperatures, varying monolayer ligands and alloys and (d) isolate and characterize $Au_{130-x}Ag_x(SR)_{50}$.

MS data based core size conversion and the proposed mechanism. In Scheme 2, the starting material represents the polydisperse clusters larger than 40 kDa, which is the 0 h sample shown in Fig. 1. When this product is etched with excess ligand, mass spectrometry analysis of the samples collected at different time intervals shows the accumulation of $Au_{130}(SR)_{50}$ in the reaction mixture over time. This mass spectrometry data provide clear evidence that the larger clusters (>40 kDa) are core converted to $Au_{130}(SR)_{50}$ during etching. During these reactions 76.3 kDa nanomolecule is also observed due to its high stability. During etching, Au–SR aggregates are the expected by-products. However, the by-products in the etching of alloy clusters might be different and needs further studies.

For the formation of $Au_{130}(SR)_{50}$, larger nanoclusters should breakdown in size. One possible route for this is the removal of metal atoms and ligands from the surface of the larger clusters. This process continues until the $Au_{130}(SR)_{50}$ is formed in the reaction. However not all the larger clusters undergo this process. Highly stable species like the 76.3 kDa nanomolecule stays unaltered in the reaction mixture. Only the meta-stable species undergo this core conversion process. After the surface

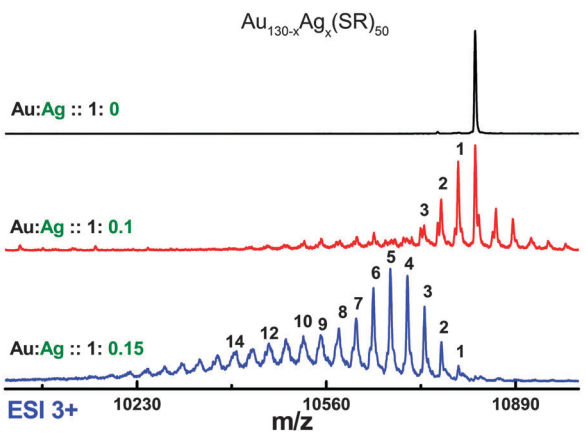

Fig. 3 Positive mode ESI MS of 3+ peaks for two different Au : Ag precursor ratios. Upon increasing the Au : Ag ratio to 1 : 0.15, $Au_{125}Ag_5(SCH_2CH_2Ph)_{50}$ is the major peak observed.

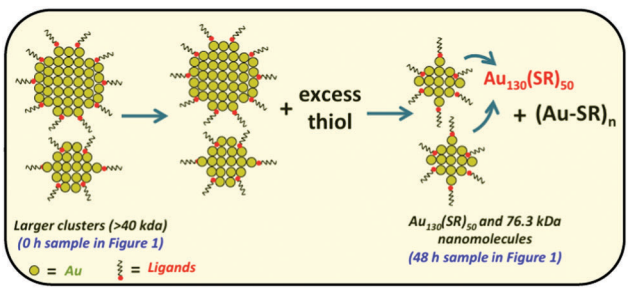

Scheme 2 Core size conversion of larger nanoclusters to form $Au_{130}(SR)_{50}$. A breakdown–reaggregation approach where the metal atoms and ligands recombine with nanomolecules to form monodisperse nanomolecules.

metal atoms and ligands are removed from the larger clusters, the remaining ligands and gold atoms might rearrange to increase the structural and geometrical stability to form $Au_{130}(SR)_{50}$. However, based on the experimental evidence obtained from these experiments, this is only a proposed mechanism. $Au_{38}(SR)_{24}$ formed in etching experiments is also a result of core conversion.[12,13] Recent reports on Au_{36} metal atom nanomolecules show that Au_{36} is not present in the initial products and is a result of core size conversion of clusters larger than Au_{36}.[28,29] In both the cases, Au_{36} and Au_{130} studied in this work, the larger clusters core convert to smaller nanomolecules.

III. Characterization of $Au_{130}(SR)_{50}$ and $Au_{130-x}Ag_x(SCH_2CH_2Ph)_{50}$ nanomolecules

Pure samples obtained after SEC were further used for characterization by several techniques. Mass spectrometry techniques, MALDI-MS[30] and high resolution ESI-MS,[31] were used to find the composition of the nanomolecules. Mass spectrometry of the nanomolecule with several ligands, shown in Fig. 2, further confirmed the composition.

Fig. 4 shows the UV-vis spectrum of $Au_{130}(SCH_2CH_2Ph)_{50}$ in comparison with $Au_{130-x}Ag_x(SCH_2CH_2Ph)_{50}$ and $Au_{130}(SC_6H_{13})_{50}$. $Au_{130}(SC_6H_{13})_{50}$ shows the same UV-vis absorption features as $Au_{130}(SCH_2CH_2Ph)_{50}$. The onset of absorbance is at 800 nm typical for gold nanomolecules.[32] With decreasing wavelength there is an increase in the absorbance. For $Au_{130}(SR)_{50}$ three major absorbance peaks were observed at 360 nm, 507 nm and 708 nm. The absorption features at ~500 nm and ~700 nm were also observed in $Au_{130}(SR)_{50}$ reported by Negishi.[16]

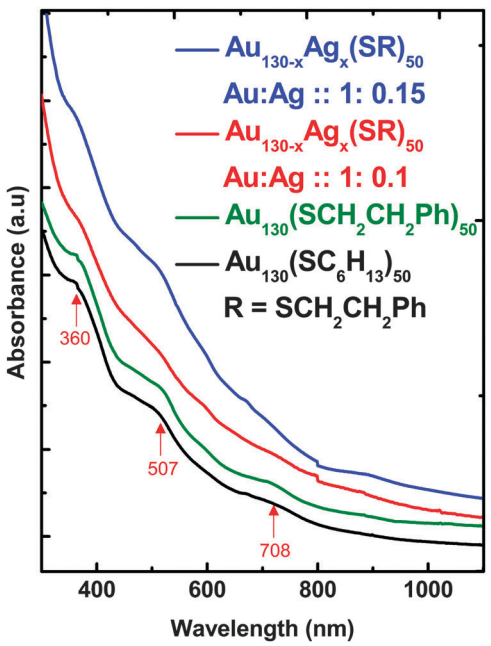

Fig. 4 UV-vis spectrum of $Au_{130}(SR)_{50}$ (red) in comparison with $Au_{130-x}Ag_x(SR)_{50}$ (red and blue). Pure Au_{130} with both phenylethanethiol and hexanethiol show the same absorption features. Upon silver incorporation, the absorbance features are not as prominent and show a monotonous absorption spectrum.

No surface plasmon resonance (SPR) peak was observed which agrees with the size transition expected. For $Au_{130-x}Ag_x(SR)_{50}$, the absorbance features are not as prominent as $Au_{130}(SR)_{50}$. A similar scenario was also observed for $Au_{38-x}Ag_x(SR)_{24}$, where the optical features were diminished upon silver atom incorporation. Recently, theoretical calculations were used to study the optical features of $Au_{144-x}Ag_x(SR)_{60}$ at different silver atom incorporations.[33] It is shown that the random alloying of silver atoms can break the degeneracy of the electronic states and cause spreading of the electronic states. Such an effect would result in monotonous absorbance features with no distinct shapes. The absorbance spectrum of $Au_{130}(SR)_{50}$ is compared with that of $Au_{144}(SR)_{60}$ and $Au_{137}(SR)_{56}$ in Fig. S7 in the ESI.†

Atomic structure. Mass spectrometry data have given the exact atomic composition of the nanomolecule. The atomic structure of the nanomolecule can be studied using X-ray diffraction data.[34,35] Single crystal diffraction data give the location of the atoms in a crystal lattice. However, it is very difficult to obtain single crystals of gold nanomolecules, especially for those larger than ~100 gold atoms. In such cases, powder X-ray diffraction is used to get an estimate of the core metallic structure of the nanomolecule. Fig. 5 shows the powder X-ray diffraction data obtained for the $Au_{130}(SR)_{50}$ nanomolecule in comparison with that of $Au_{67}(SR)_{35}$ (ref. 36) and the 76.3 kDa cluster. The diffraction pattern best matches with Au_{67} which was proposed to contain a Marks decahedral core. Decahedra possess a five-fold symmetry and are formed by packing of five regular tetrahedrons.[37] These tetrahedrons need to be slightly distorted to accommodate into a decahedral structure. Such distortions induce internal strain on the structure. The diffraction pattern of the 76.3 kDa nanomolecule is included in the figure to prove the contrast between the fcc diffraction pattern and observed diffraction for the $Au_{130}(SR)_{50}$ nanomolecule.

Powder XRD data suggest that the nanomolecule has Marks decahedral geometry. Supported by the powder XRD data and

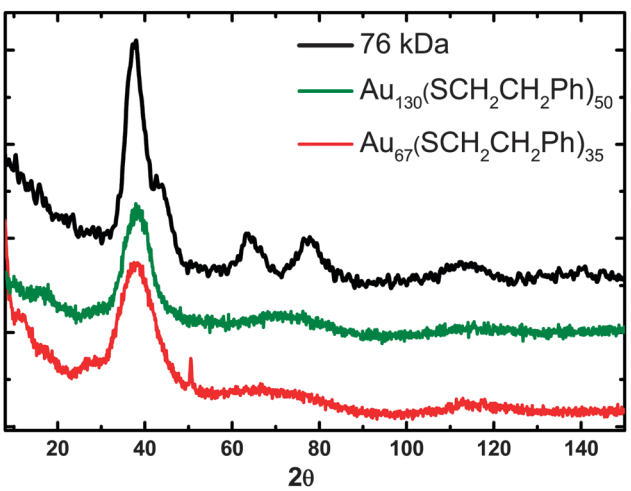

Fig. 5 Powder X-ray diffraction of $Au_{130}(SR)_{50}$ in comparison with $Au_{67}(SR)_{35}$ and 76.3 kDa nanomolecules, suggesting a Marks decahedral core for the 130-atom title compound.

oblate structure observed in TEM, Negishi's group has proposed a similar structure for this nanomolecule.[16] Recently Whetten and coworkers[38] have also proposed a structure based on theoretical calculations, which agrees with the one proposed by Negishi earlier. The proposed structure consists of a 105-atom core, which can be broken down into a 75 atom Marks decahedron covered by 15 atom caps on top and bottom. This structure shows a five-fold symmetry axis. The remaining gold atoms are present on the surface in the form of 25 –[SR–Au–SR]– short staples. With the given atomic composition the nanomolecule would have 80 valence electrons. However this does not form a closed electronic shell according to the spherical jellium model.[39,40] However, nanomolecules with non-spherical cores, like Au_{38}, and Au_{67}, are found to be stable in the reaction mixtures.[36,41–43] This shows that the electron shell closing values for prolated and elongated structures are different than the values anticipated by the spherical jellium model. The proposed structural model should be further confirmed by growing single crystals of this nanomolecule. Efforts are being made in this direction.

Conclusions

For the first time, the concept of core size conversion in larger clusters with >200 metal atoms to form $Au_{130}(SR)_{50}$ is proven using mass spectrometry evidence. Using a scalable synthetic protocol $Au_{130}(SR)_{50}$ and $Au_{130-x}Ag_x(SR)_{50}$ were synthesized *via* the core size conversion process and characterized in detail. The process of core size conversion is repeated using different ligands to check the validity of the process. A few insights into the mechanism of core conversion are also presented here which would facilitate the understanding of the core conversion process and has a broader impact. The established synthesis, characterization and high stability of $Au_{130}(SR)_{50}$ make it a potential candidate for several applications. However, much needs to be understood about its structure. This needs further theoretical and experimental studies. Using the established protocol, the synthesis is scaled up to obtain larger quantities of pure $Au_{130}(SCH_2CH_2Ph)_{50}$ and crystallization attempts are under way.

Acknowledgements

We gratefully acknowledge support from the NSF 1255519 and NSF 0903787. We thank the reviewers for suggestions that significantly improved this manuscript.

References

1 M.-C. Bowman, T. E. Ballard, C. J. Ackerson, D. L. Feldheim, D. M. Margolis and C. Melander, *J. Am. Chem. Soc.*, 2008, **130**, 6896.
2 C.-A. J. Lin, T.-Y. Yang, C.-H. Lee, S. H. Huang, R. A. Sperling, M. Zanella, J. K. Li, J.-L. Shen, H.-H. Wang, H.-I. Yeh, W. J. Parak and W. H. Chang, *ACS Nano*, 2009, **3**, 395.
3 W. Chen and S. Chen, *Angew. Chem., Int. Ed.*, 2009, **48**, 4386.
4 P. K. Jain, X. Huang, I. H. El-Sayed and M. A. El-Sayed, *Acc. Chem. Res.*, 2008, **41**, 1578.
5 G. Schmid, M. Baumle, M. Geerkens, I. Heim, C. Osemann and T. Sawitowski, *Chem. Soc. Rev.*, 1999, **28**, 179.
6 R. L. Whetten, J. T. Khoury, M. M. Alvarez, S. Murthy, I. Vezmar, Z. L. Wang, P. W. Stephens, C. L. Cleveland, W. D. Luedtke and U. Landman, *Adv. Mater.*, 1996, **8**, 428.
7 M. Brust, M. Walker, D. Bethell, D. J. Schiffrin and R. Whyman, *J. Chem. Soc., Chem. Commun.*, 1994, 801.
8 K. Edinger, A. Goelzhaeuser, K. Demota, C. Woell and M. Grunze, *Langmuir*, 1993, **9**, 4.
9 T. G. Schaaff and R. L. Whetten, *J. Phys. Chem. B*, 1999, **103**, 9394.
10 M. J. Hostetler, S. J. Green, J. J. Stokes and R. W. Murray, *J. Am. Chem. Soc.*, 1996, **118**, 4212.
11 R. S. Ingram, M. J. Hostetler, R. W. Murray, T. G. Schaaff, J. T. Khoury, R. L. Whetten, T. P. Bigioni, D. K. Guthrie and P. N. First, *J. Am. Chem. Soc.*, 1997, **119**, 9279.
12 N. K. Chaki, Y. Negishi, H. Tsunoyama, Y. Shichibu and T. Tsukuda, *J. Am. Chem. Soc.*, 2008, **130**, 8608.
13 H. Qian, Y. Zhu and R. Jin, *ACS Nano*, 2009, **3**, 3795.
14 R. Jin, H. Qian, Z. Wu, Y. Zhu, M. Zhu, A. Mohanty and N. Garg, *J. Phys. Chem. Lett.*, 2010, **1**, 2903.
15 A. Dass, *J. Am. Chem. Soc.*, 2011, **133**, 19259.
16 Y. Negishi, C. Sakamoto, T. Ohyama and T. Tsukuda, *J. Phys. Chem. Lett.*, 2012, **3**, 1624.
17 Z. Tang, D. A. Robinson, N. Bokossa, B. Xu, S. Wang and G. Wang, *J. Am. Chem. Soc.*, 2011, **133**, 16037.
18 S. Knoppe, J. Boudon, I. Dolamic, A. Dass and T. Burgi, *Anal. Chem.*, 2011, **83**, 5056.
19 J. M. Pettibone and J. W. Hudgens, *ACS Nano*, 2011, **5**, 2989.
20 H. Qian, Y. Zhu and R. Jin, *Proc. Natl. Acad. Sci. U. S. A.*, 2012, **109**, 696.
21 R. A. Lordeiro, F. F. Guimarães, J. C. Belchior and R. L. Johnston, *Int. J. Quantum Chem.*, 2003, **95**, 112.
22 R. Ferrando, J. Jellinek and R. L. Johnston, *Chem. Rev.*, 2008, **108**, 845.
23 C. Kumara and A. Dass, *Nanoscale*, 2011, **3**, 3064.
24 C. Kumara and A. Dass, *Nanoscale*, 2012, **4**, 4084.
25 Y. Negishi, K. Munakata, W. Ohgake and K. Nobusada, *J. Phys. Chem. Lett.*, 2012, **3**, 2209.
26 Y. Negishi, K. Igarashi, K. Munakata, W. Ohgake and K. Nobusada, *Chem. Commun.*, 2012, **48**, 660.
27 H. Qian, D.-e. Jiang, G. Li, C. Gayathri, A. Das, R. R. Gil and R. Jin, *J. Am. Chem. Soc.*, 2012, **134**, 16159.
28 P. R. Nimmala and A. Dass, *J. Am. Chem. Soc.*, 2011, **133**, 9175.
29 C. Zeng, H. Qian, T. Li, G. Li, N. L. Rosi, B. Yoon, R. N. Barnett, R. L. Whetten, U. Landman and R. Jin, *Angew. Chem., Int. Ed.*, 2012, **51**, 13114.
30 A. Dass, A. Stevenson, G. R. Dubay, J. B. Tracy and R. W. Murray, *J. Am. Chem. Soc.*, 2008, **130**, 5940.
31 J. B. Tracy, M. C. Crowe, J. F. Parker, O. Hampe, C. A. Fields-Zinna, A. Dass and R. W. Murray, *J. Am. Chem. Soc.*, 2007, **129**, 16209.

32 M. M. Alvarez, J. T. Khoury, T. G. Schaaff, M. N. Shafigullin, I. Vezmar and R. L. Whetten, *J. Phys. Chem. B*, 1997, **101**, 3706.
33 J. Koivisto, S. Malola, C. Kumara, A. Dass, H. Hakkinen and M. Pettersson, *J. Phys. Chem. Lett.*, 2012, **3**, 3076.
34 R. L. Whetten, M. N. Shafigullin, J. T. Khoury, T. G. Schaaff, I. Vezmar, M. M. Alvarez and A. Wilkinson, *Acc. Chem. Res.*, 1999, **32**, 397.
35 C. L. Cleveland, U. Landman, T. G. Schaaff, M. N. Shafigullin, P. W. Stephens and R. L. Whetten, *Phys. Rev. Lett.*, 1997, **79**, 1873.
36 P. R. Nimmala, B. Yoon, R. L. Whetten, U. Landman and A. Dass, *J. Phys. Chem. A*, 2013, **117**, 504.
37 F. Baletto and R. Ferrando, *Rev. Mod. Phys.*, 2005, **77**, 371.
38 A. Tlahuice-Flores, U. Santiago, D. Bahena, E. Vinogradova, C. V. Conroy, T. Ahuja, S. B. H. Bach, A. Ponce, G. Wang, M. Jose-Yacaman and R. L. Whetten, *J. Phys. Chem. A*, 2013, **117**, 10470.
39 M. Walter, J. Akola, O. Lopez-Acevedo, P. D. Jadzinsky, G. Calero, C. J. Ackerson, R. L. Whetten, H. Gronbeck and H. Hakkinen, *Proc. Natl. Acad. Sci. U. S. A.*, 2008, **105**, 9157.
40 T. P. Martin, T. Bergmann, H. Goehlich and T. Lange, *J. Phys. Chem.*, 1991, **95**, 6421.
41 H. Qian, W. T. Eckenhoff, Y. Zhu, T. Pintauer and R. Jin, *J. Am. Chem. Soc.*, 2010, **132**, 8280.
42 P. D. Jadzinsky, G. Calero, C. J. Ackerson, D. A. Bushnell and R. D. Kornberg, *Science*, 2007, **318**, 430.
43 A. Dass, P. R. Nimmala, V. R. Jupally and N. Kothalawala, *Nanoscale*, 2013, **5**, 12082–12085.